Inhomogeneous broadening in spectral bands of carbonmonoxymyoglobin

The connection between spectral and functional heterogeneity

P. Ormos,*‡ A. Ansari,* D. Braunstein,* B. R. Cowen,* H. Frauenfelder,* M. K. Hong,* I. E. T. Iben,* T. B. Sauke,* P. J. Steinbach,* and R. D. Young*§

*Departments of Physics and Biophysics, University of Illinois, Urbana, Illinois 61801; ‡Institute of Biophysics, Hungarian Academy of Sciences, Szeged, Hungary; and §Department of Physics, Illinois State University, Normal, Illinois 61761

ABSTRACT The rebinding kinetics of CO to myoglobin after flash photolysis is nonexponential in time below ~180 K; the kinetics is governed by a distribution of enthalpic barriers. This distribution results from inhomogeneities in the protein conformation, referred to as conformational substates. Hole-burning experiments on the Soret and IR CO-stretch bands test the assumption that an inhomogeneous distribution of conformational substates results in inhomogeneously broadened spectra. CO was slowly photolyzed at different wavelengths in the Soret band at 10 K. Both the Soret band and the CO-stretch band A_1, centered at 1,945 cm^{-1}, shift during photolysis, demonstrating that different wavelengths excite different parts of the distributed population. We have also done kinetic hole-burning experiments by measuring peak shifts in the Soret and A_1 bands as the CO molecules rebind. The shifts indicate that the spectral and enthalpic distributions are correlated. In the A_1 band, the spectral and enthalpic distributions are highly correlated while in the Soret the correlation is weak. From the peak shifts in the spectral and kinetic hole-burning experiments the inhomogeneous broadening is estimated to be ~15% of the total width in the Soret band and ~60% in A_1. We have previously measured the tilt angle α between the bound CO and the heme normal (Ormos, P., D. Braunstein, H. Frauenfelder, M. K. Hong, S.-L. Lin, T. B. Sauke, and R. D. Young. 1988. *Proc. Natl. Acad. Sci. USA.* 85:8492–8496) and observed a wave number dependence of the tilt angles within the CO-stretch A bands. Thus the spectral and enthalpic distributions of the A bands are coupled to a heterogeneity of the structure.

INTRODUCTION

Proteins are highly complex systems; the complexity is a direct consequence of their construction (1–3). Proteins do not fold into a unique tertiary structure, but can assume a large number of slightly different structures, called conformational substates (CS) (1, 4–6). The conformational energy landscape of a protein consists of many energy valleys separated by barriers (Fig. 1). The valleys are the CS. Protein molecules in different CS perform the same function, but possibly with different rates (5, 7). Other complex systems such as glasses (8) and spin glasses (9–11) also have a conformational energy landscape exhibiting a large number of valleys.

Various experiments imply that CS are arranged in a hierarchy of several tiers (7, 12). We denote with CS^i, i = 0,1, . . . substates of tier 0,1, . . . , arranged by decreasing barrier heights between substates. Two tiers, CS^0 and CS^1, are shown in Fig. 1. At least three substates of tier 0 are observed in MbCO; they are characterized by their CO stretch frequency (7, 13, 14) and by the tilt angle between the heme normal and the bound CO (15, 16). The three CS^0 substates, denoted by A_0, A_1, and A_3 in Fig. 1, rebind CO with different rates (7, 17). Rebinding in each CS^0 is nonexponential in time, indicating that each CS^0 consists of a large number of CS^1 as also sketched in Fig. 1. The next lower tier of substates, CS^2, is suggested by Mössbauer effect data (18) and by flash photolysis experiments after prolonged illumination (7, 19).[1] The inelastic neutron scattering (23) and the specific heat data on metmyoglobin (24) are evidence for even lower tiers of substates. The nonphotochemical hole burning in apomyoglobin also demonstrates the heterogeneity of the structure at low energy levels (25), but on a nonnative system.

At physiological temperatures proteins fluctuate among substates of all tiers. As the temperature is lowered, transitions between substates become slower. In a glycerol–water solvent, transitions among CS^0 freeze out at ~180 K, among CS^1 at ~160 K (26). Transitions

A. Ansari's present address is National Institutes of Health, 9000 Rockville Pike, Bethesda, MD; M. K. Hong's present address is Department of Physics, Princeton University, Princeton, NJ; I. E. T. Iben's present address is AT&T Bell Laboratories, Murray Hill, NJ; T.B. Sauke's present address is NASA Ames Research Center, Moffet Field, CA.

[1] In reference 10 we erroneously took the shift of the near-IR band in Mb near 760 nm (band III) as evidence for substates of tier 2. Agmon suggested that kinetic hole burning might be the reason of the apparent shift during rebinding (20). This mechanism has been verified by Campbell et al. (21) and by Ansari (22). Nevertheless, CS^2 appear to be present (7, 18, 19).

0006-3495/90/02/191/09 $2.00

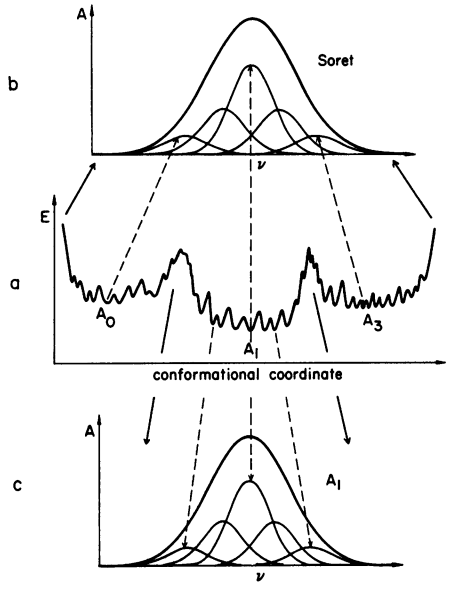

FIGURE 1 Origin of inhomogeneous broadening of the Soret and infrared A bands of MbCO. (*a*) Schematic conformational energy landscape of MbCO. The three well-defined valleys represent the A substates characterized by infrared spectroscopy. (*b* and *c*) The consequent inhomogeneous broadening of the absorption spectrum. Note that while the Soret band is characteristic of the whole protein population, the A_1 infrared band is characteristic only of a subpopulation.

among CS^2 become very slow near 160 K (7). The protein thus experiences successive glass transitions as fluctuations in the various tiers freeze out. Below 160 K, for example, a given protein molecule will remain frozen in a particular substate CS^1 within a particular substate CS^0(26), but fluctuations among CS^2 may still occur. The protein ensemble is then a static population of molecules in various CS^0 and CS^1. Indeed, structural heterogeneity is seen in the Debye–Waller factor in x-ray crystallography (1, 3, 4, 27, 28). If the structural characteristics of the protein are different in the different CS, the observed bands should also reflect the heterogeneity. An inhomogeneous broadening of the absorption spectrum due to distributed protein–pigment interactions in rhodopsin was suggested earlier by Cooper (29). Based on Cooper's ideas we demonstrated and determined the inhomogeneous broadening of the main absorption band of bacteriorhodopsin (30). Srajer et al. showed the Soret band of Mb to be inhomogeneously broadened (31). Here we demonstrate that spectral and kinetic hole-burning experiments provide evidence for inhomogeneous broadening of the spectrum of MbCO and yield insight into the relationship between the function and the dynamic structure of proteins by connecting functional, spectroscopic, and structural properties (15, 32).

We employ two spectroscopic markers, the IR stretch bands of the bound CO in carbonmonoxymyoglobin (MbCO) and the Soret band in the visible region of MbCO. There are three major CO stretch bands in MbCO, A_0 at 1,966 cm^{-1}, A_1 at 1,945 cm^{-1}, and A_3 at 1,933 cm^{-1} (7, 13). These bands are assigned to three different CS^0 called A_0, A_1, and A_3 which we interpret as three slightly different protein conformations (14, 15). Here we concentrate on A_1, the most intense band at pH 7 (7).

The functional marker comes from low-temperature flash photolysis experiments (5–7). After photodissociation at temperatures below ~160 K, the CO remains in the heme pocket B. The resulting CO stretch bands are identified as B substates and are blue-shifted from those of the A substates. Rebinding in each of the pathways $B \rightarrow A$ is nonexponential in time (7, 33). Rebinding monitored in the Soret band is also nonexponential in time (5) and probes a combination of the individual pathways $B \rightarrow A$ (7, 34). The nonexponential time course for rebinding is explained by assuming that proteins in different conformational substates have different enthalpic barriers, with $g(H)dH$ denoting the probability of a protein having an enthalpic barrier between H and $H + dH$. The fraction of Mb molecules that have not rebound a CO at time t after photodissociation is given by

$$N(t) = \int g(H) \exp[-k(H)t]dH, \quad (1)$$

where $k(H) = A \exp(-H/RT)$ and the preexponential A depends on the entropic barrier. The distribution $g(H)$ is characteristic of the static distribution of proteins over the CS^1 and provides the functional marker.

MATERIALS AND METHODS

Spectral hole-burning

The existence of substates with different properties results in an inhomogeneous broadening of the spectral lines of a protein ensemble. The experimental technique used to observe this broadening is analogous to the hole burning of dyes embedded in heterogeneous glass matrices (35) and is an adaptation of the experiments and evaluation used to demonstrate the inhomogeneous broadening of the absorption spectrum of bacteriorhodopsin (30). These spectral hole-burning experiments employ selective photolysis: In the linear photolysis regime where the number of proteins photolyzed is proportional to the number of photons, light of different wavelengths will photolyze different populations of the protein ensemble depending on the absorption coefficients at the excitation wavelength. The resulting spectra have slightly different shapes. The situation is illustrated in Fig. 2 *a*. If the protein sample is photolyzed in successive small steps and the spectra are measured after each step, the difference spectra between successive steps will shift. Excitation wavelengths were chosen in the Soret band of MbCO, and the spectral hole burning was monitored in both the Soret (method 1) and infrared A_1 band (method 2) of MbCO. The protein sample was cooled to 10 K, where CO rebinding to Mb is negligible on the time scale of these experiments.

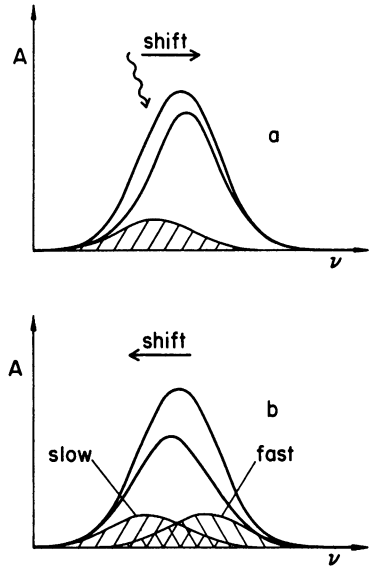

FIGURE 2 Schematic representation of the two hole-burning techniques. (*a*) Spectral hole-burning (methods 1 and 2). The band is excited on the low-frequency side. The solid curve represents the observed band; the cross-hatched area represents one of the many underlying bands. The protein ensemble is photodissociated preferentially on the low frequency side causing a shift in the observed band. (*b*) Kinetic hole-burning (methods 3 and 4). The cross-hatched areas represent two components with different rebinding rates. The case illustrated is for the A_1 band: the high-frequency components bind faster, resulting in a shift of the peak to lower frequency. In the Soret band, the low-frequency side binds faster, resulting in a shift to higher frequency.

Kinetic hole-burning

If a spectral distribution is nonrandomly mapped onto the distribution of enthalpic barriers $g(H)$, the spectrum changes shape during rebinding of CO to Mb after photodissociation (37). In other words, if different populations of the ensemble of Mb molecules rebind with different rates and have slightly different absorption spectra (Fig. 2 *b*), the difference spectra will shift in time. This effect is known as kinetic hole-burning (20, 21). Rebinding was monitored both in the Soret band (method 3) and in the infrared A_1 band (method 4) of MbCO. The protein sample was cooled to 40 K, where rebinding occurs on a convenient time scale for these kinetic hole-burning experiments.

Sample preparation

Lyophilized sperm whale Mb from Sigma Chemical Co. (St. Louis, MO) was dissolved in 75% (vol/vol) glycerol/water buffered to pH 6.9 with 0.1 M potassium phosphate. The sample was stirred under a CO atmosphere for several hours, reduced with threefold excess sodium dithionite, and stirred to form MbCO. The final protein concentration was ~5 μM for the Soret experiments.

FTIR experiments

The sample was placed between two CaF_2 windows separated by a 6-μm spacer. The infrared spectra were taken on a Mattson Sirius 100 FTIR spectrophotometer with spectral resolution 1 or 0.5 cm^{-1}. At 1 cm^{-1} resolution 1,000 scans were averaged, and at 0.5 cm^{-1} resolution 500 scans were averaged. Both cases resulted in ~600 s scanning time. In the kinetic experiments at the earliest times, the number of scans was reduced to improve temporal resolution. The sample temperature was controlled with a closed-cycle helium refrigerator (model 21; CTI-Cryogenics Div., Waltham, MA) and varied between 10 K and 300 K.

Soret experiments

Spectra in the visible were collected with a Cary-14 spectrophotometer upgraded by OLIS (Atlanta, GA) with a nominal spectral resolution of 0.1 nm. The sample was kept in a 10-mm plastic cuvette. Temperature was controlled with a liquid He storage dewar (Janis Research Co., Wilmington, MA) and a temperature controller (Lake-Shore Cryogenics Inc., Westerville, OH) between 5 and 300 K.

Photolysis

The sample was illuminated with either white or monochromatic light. White-light excitation was achieved with a 250-W tungsten lamp (Oriel Corp., Stamford, CT). The light was focused on the sample after passing through a 15-cm pathlength water heat filter. Monocromatic light was obtained from a 75-W Xenon lamp (Oriel Corp.) and passed through a monochromator (Jarrel-Ash, Waltham, MA). The band width of the exciting light was ~1nm.

RESULTS AND DATA EVALUATION

Method 1: spectral hole-burning in the Soret, monitored in the Soret

MbCO was photolyzed in successive small steps with light of two different wavelengths, and the spectrum was measured after each illumination. The photolyzing wavelengths were 417 and 431 nm, where the slope of the Soret band has the largest magnitude, and therefore the largest difference between the spectra resulting from the two excitations is expected. If the band is inhomogeneously broadened, the difference spectra $A(n) - A(0)$ shift as the photolysis proceeds. Here $A(n)$ represents the spectrum after the nth photolysis step and $A(0)$ is the initial spectrum. If excitation occurs at the low-wavelength slope, then the difference spectra shift from lower to higher wavelengths. Fig. 3 shows the peak regions of the difference spectra that result while photolyzing the first and second half of the population, respectively. The opposite and symmetric shifts in the case of excitation light at 417 and 431 nm prove that the Soret band is inhomogeneously broadened. The small size of the shift suggests a narrow inhomogeneous width. The method of Rousseau (38) was used to determine the shift: If the shift of the peak is much smaller than the line width of the band, then the difference of the spectra before and after the shift has the shape of the peak's derivative and its amplitude is proportional to the shift. By comparing the

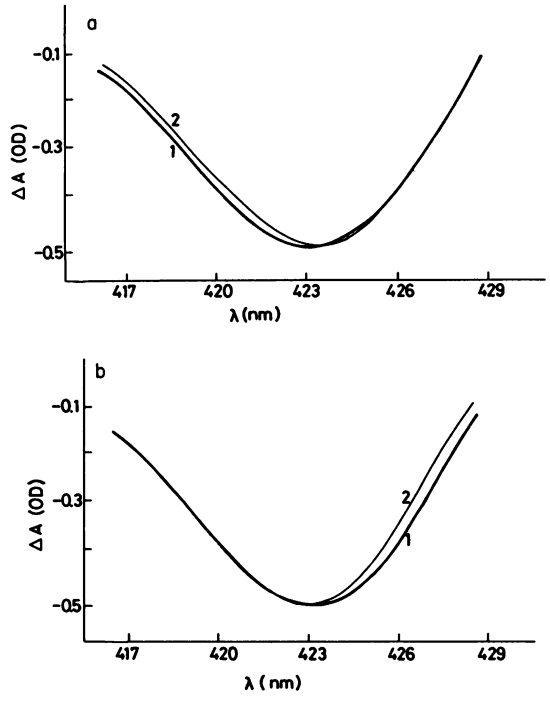

FIGURE 3 The peak regions of the Soret difference spectra (Mb-MbCO) after different amounts of photolysis at 10 K. The difference spectra are normalized. 1: A = $A(50\%)$ − $A(0\%)$, 2: A = $A(100\%)$ − $A(50\%)$. The percentages give the fraction that has been photolyzed. (*a*) Excitation at 417 nm; (*b*) Excitation at 432 nm.

amplitude of the difference spectrum to the amplitude of the shifting band, the shift can be determined. Here and in the following, this method was applied to obtain all spectral shifts. In the data presented in Fig. 3 the shift between the difference spectra is 0.18 nm.

Method 2: spectral hole-burning in the Soret, monitored in the IR CO stretch band A_1 of MbCO

The experiment is similar to that described in the previous section: If the A_1 band is inhomogeneously broadened owing to the distribution of protein properties that affect binding and if there is a correlation between the Soret and IR spectral distributions, then by following a photolysis sequence as described above the absorption difference spectra of the A_1 band should also show a shift. The experiment was performed with photolysis light of 415 and 432 nm wavelength. Fig. 4 shows data with the largest initial shifts. The difference in position of the difference spectra at small (~20%) photolysis between 415 and 432 nm excitation is 0.2 cm^{-1}. The result proves that the A_1 band is inhomogeneously broadened and that

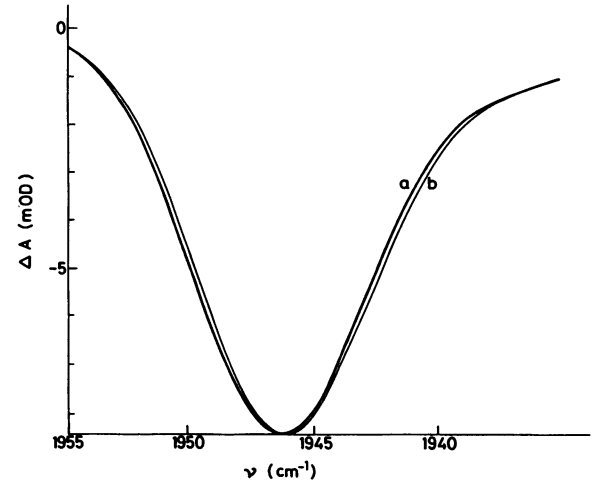

FIGURE 4 Infrared difference spectra (Mb-MbCO) in the A_1 stretch frequency region of bound CO after 20% of MbCO was photolyzed at 10 K. (*a*) Photolysis at 417 nm. (*b*) Photolysis at 432 nm.

the low (high) frequencies of the Soret band correspond to low (high) frequencies of the infrared A_1 band.

Method 3: kinetic hole-burning in the Soret band

Fig. 5 *b* shows the difference spectra $[A(t) - A(0)]$, where $A(t)$ is the absorbance at different times t after photolysis with white light at 40 K. $A(0)$ is the absorbance before the flash (Fig. 5 *a*). To demonstrate and determine the shift, first the successive difference spectra were normalized to each other, then the first one was subtracted from the later ones. Fig. 5 *c* shows these differences, characteristic of shifts in both the MbCO and photodissociated Mb bands. From 60 to 15 × 10^3 s the difference spectrum for the MbCO band shifted by 0.6 nm to larger frequencies. The shift of the photodissociated Mb band also shows kinetic hole-burning, consistent with the results of Šrajer et al. (31).

Method 4: kinetic hole-burning in the A_1 band

MbCO was photolyzed with white light at 40 K and rebinding was followed in the infrared A bands. Fig. 6 shows the difference spectra $[A(t) - A(0)]$ in the bound CO stretch-frequency region. The spectra show the "missing" bound ligands at different times. The shift during rebinding is best seen in the case of the A_1 band, which moves to lower frequencies. The spectra taken 10 s and 3 × 10^4 s after flash-off differ by 1 cm^{-1}. The width of the difference spectrum increases from 7.7 cm^{-1} at 10 s to 8.8 cm^{-1} at 3 × 10^4 s.

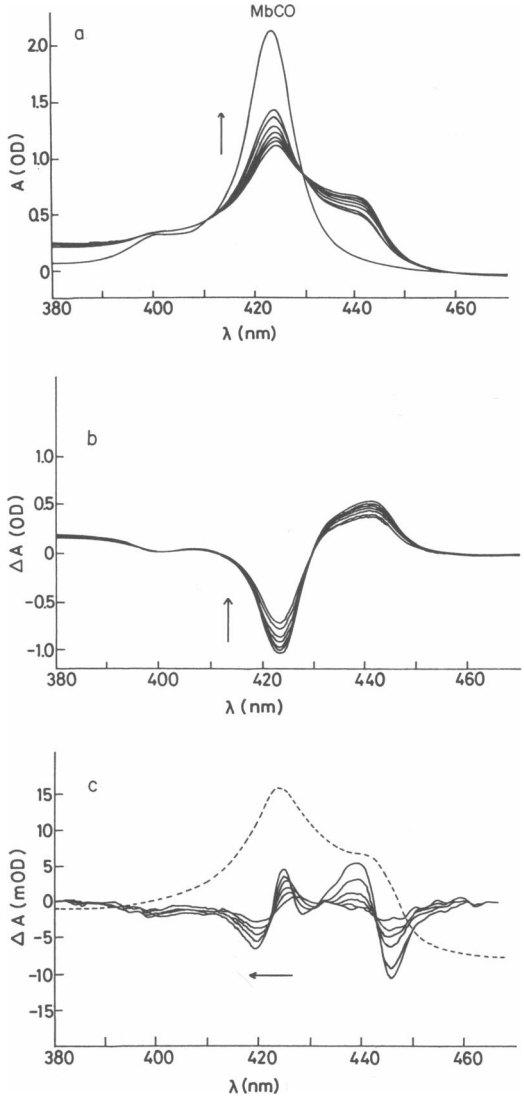

FIGURE 5 Shift of the Soret band of MbCO during rebinding of CO after photolysis at 40 K. (*a*) Successive absorption spectra. The spectra were taken in logarithmically increasing intervals after photolysis; the first and last spectra represent $t = 30$ s and $t = 30 \times 10^4$ s after illumination, respectively. The arrow indicates the direction of absorption changes during rebinding. (*b*) The successive Mb-MbCO difference spectra. (*c*) The difference of the difference spectra in *b* after normalization. The first difference spectrum is subtracted from the later ones. The arrow indicates the direction of the shift of the Soret band of MbCO during rebinding. The shift in the Soret band of photodissociated Mb during rebinding is also shown. The dashed line shows a spectrum of partially photolyzed MbCO to locate the position of the peaks due to MbCO and Mb.

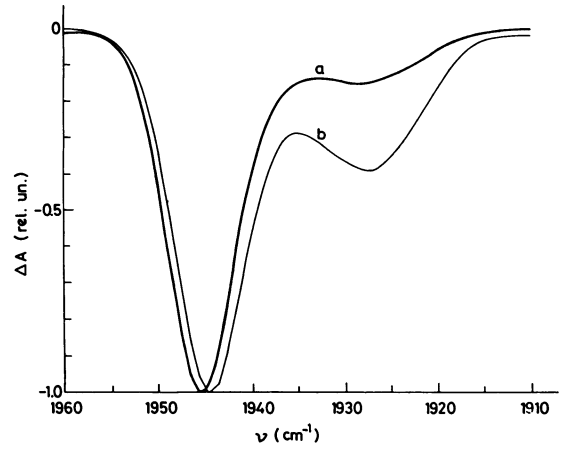

FIGURE 6 The shift of the A_1 (Mb-MbCO) difference spectrum during rebinding of CO after photolysis at 40 K. (*a*) The difference spectrum at $t = 10$ s after photolysis. (*b*) The difference spectrum at $t = 3 \times 10^4$ s after photolysis. The difference spectra are normalized to each other to demonstrate the shift. The apparent growth of A_3 is due to the slower CO rebinding in A_3.

Homogeneous and inhomogeneous line widths

All the data presented point to inhomogeneous broadening of the spectral bands of MbCO. The four different hole-burning experiments are spectroscopic markers of different properties and represent distributions along different protein coordinates. In the spectral hole-burning monitored in the Soret band (method 1), the inhomogeneous broadening is directly responsible for the observed shift. In the other three experiments, the selective perturbation is achieved along a distribution different from the one observed. In the spectral hole-burning with IR monitoring (method 2) the selective photolysis is performed along the Soret spectral distribution. The shift and the inhomogeneous broadening of the A_1 band is caused by the coupling of the spectral distributions in the Soret and the IR. Similarly, in the kinetic hole-burning experiments (methods 3 and 4) the shift is determined by the distribution of the bands, the distribution of enthalpic barriers $g(H)$, and their mapping onto each other.

In order to estimate the homogeneous and inhomogeneous widths for the Soret and A_1 bands, we characterize the correlations described in the preceding paragraph in the following way: The protein substates of tiers 0, 1, and 2 (CS^0, CS^1, and CS^2) do not interconvert up to 40 K, the highest temperature of our experiments, indicating the absence of structural relaxations involving these tiers (7, 17, 21, 22). Consequently, the observed spectral bands are frozen into static distributions. We simulate the line shapes of the observed bands by expressing them as superpositions of many slightly shifted bands. We performed the simulation with two line shapes. First, the spectra were approximated with a Gaussian distribution of Gaussian line shapes in wave number space:

$$A(\nu) = A(\nu_0) \int D(\nu', \nu_0) S(\nu, \nu') d\nu', \qquad (2)$$

where

$$D(\nu', \nu_0) = \frac{1}{\sqrt{2\pi}\omega_{ih}} \exp\left(-\frac{(\nu' - \nu_0)^2}{2\omega_{ih}^2}\right) \quad (3)$$

and

$$S(\nu, \nu') = \frac{1}{\sqrt{2\pi}\omega_h} \exp\left(-\frac{(\nu - \nu')^2}{2\omega_h^2}\right). \quad (4)$$

Here ω_{ih} is the inhomogeneous and ω_h the homogeneous width. $D(\nu', \nu_0)$ is the inhomogeneous broadening and $S(\nu, \nu')$ is the homogeneous spectrum. In the numerical simulation the spectra were modeled as a sum of 11 Gaussians $S(\nu, \nu')$, whose amplitudes at $t = 0$ are Gaussian distributed by $D(\nu', \nu_0)$. In modeling the spectral hole-burning, we assumed wave-length–independent quantum yield. Hence, the reaction was simulated by taking the probability of absorbing a photon by a particular subpopulation of proteins to be proportional to the absorption of that population at the exciting wave number. In the case of the spectral hole-burning experiment where the A_1 band was monitored, we assumed that the inhomogeneous distribution of the Soret band is simply (linearly) mapped onto the distribution of the A_1 band. The mapping is not necessarily simple, and we will discuss this point in the next section.

In the simulation of the kinetic hole-burning, we assumed that the mapping between the enthalpic barrier distribution for the A_1 substate (7) was matched to the 11 spectral components according to the initial distribution of the A_1 band, and the rebinding was generated with 11 average rates. The matching was selected such that the simulation yielded peak shifts of the observed direction. In the Soret band, the low frequency side rebinds faster while in the A_1 band the high-frequency side rebinds faster.

In the simulations, pairs of homogeneous and inhomogeneous widths for the initial spectra were generated by fixing one of the widths and letting the fit determine the other. Good fits could be obtained with a wide range of widths. The simulation was then run with these different pairs of widths and the pair that resulted in the observed apparent shift of the difference spectra was selected. When simulating the spectral hole-burning monitored in the infrared A_1 band (method 2), the Soret parameters, i.e., ω_{ih} and ω_h, determined by the spectral hole-burning monitored in the Soret (method 1) were used and only the parameters of the A_1 band were varied. Table 1 gives the results of the simulation.

In addition, we performed the simulations with Voigtian line shapes, where the spectrum is a convolution of a Gaussian (the inhomogeneous distribution) and a Lorentzian (the homogeneous spectrum) (7, 39). The results of the simulations agree to within 10% for the two cases, indicating that the widths are not very sensitive to the actual line shape. The independence of the line widths of the choice of line shape is not unexpected since only peak positions were followed. In the spectral hole-burning experiments (methods 1 and 2), excitation occurred at half maximum so only the central regions of the spectra were investigated. Also, the line broadening of the difference spectrum in the IR kinetic hole-burning experiment may be the result of nonsymmetric line shapes. For symmetric spectra with symmetric distributions, one would expect a narrowing of the distribution together with a line-narrowing of the measured difference spectrum as rebinding proceeds if the population of the photolyzed distribution is "eaten away" from one side (20, 37). However, if the distribution is not symmetric, or the component spectra within the distribution do not have equal width, broadening can occur.

TABLE 1 Gaussian homogeneous and inhomogeneous line widths of MbCO

Spectral band/method*	Homogeneous width (ω_h)	Inhomogenous width‡ (ω_{ih})	ω_{ih}/ω_h
	cm^{-1}	cm^{-1}	
Soret band/method 1 (Spectral hole-burning)	269	41	0.15
Soret band/method 3 (Kinetic hole-burning)	272	13	0.05
IR A_1 band/method 2 (Spectral hole-burning)	3.7	0.7	0.19
IR A_1 band/method 4 (Kinetic hole-burning)	3.2	2	0.63

Simulation using Eqs. 2 and 3 of text.
*Methods are described in text.
‡Errors are on order of ±20%.

DISCUSSION

Conformational substates

The results presented here show that the spectral lines in MbCo that were studied, both in the visible (Soret band) and the infrared (CO stretch bands), are inhomogeneously broadened. This observation adds further support to the concept of conformational substates (5, 6). The experiments yield homogeneous line widths in the range of the total width of the bands. The hole-burning experiments result in only slight shifts of the spectra in contrast to the narrow holes observed at much lower temperatures on apomyoglobin containing cholorophyllide (25). Our experiments demonstrate the heterogeneity of the protein spectra that are frozen in the temperature range 10–40 K.

Although the rate of rebinding limits our ability to detect the effect, it may be present up to temperatures where the relaxation of CS^1 and CS^0 substates sets in, ~170–190 K (26).

Connections among spectroscopic and functional heterogeneities

Not enough information is available to connect the individual spectral and enthalpic distributions to specific protein coordinates. However, some overall features can be recognized. In the work of Champion and collaborators (31, 40), both the enthalpic barrier distribution and the inhomogeneous broadening of the Soret band of deoxy Mb are attributed to a distribution of the iron position in the heme normal direction, and the doming of the heme in the deoxy state. The data presented here indicate that the situation is more complicated. Even in MbCO, where the heme is not domed, there is a correlation between the enthalpic barrier distribution and the spectral distributions, both in the Soret and A_1 band, indicating that structural features present in the bound state are involved in the enthalpic barrier distribution. The values shown in Table 1 allow us to estimate the correlations of the distributions along the different protein coordinates. If the simple correlations assumed in the simulations using Eqs. 2 and 3 were true, the inhomogeneous widths of the Soret and the A_1 bands obtained in each pair of experiments would be equal. The total inhomogeneous width is directly measured only in the spectral hole-burning monitored in the Soret (method 1). The other methods are indirect: The selection from the inhomogeneous population of proteins is done according to a particular protein coordinate, i.e., the spectral distribution of the Soret if the effect of the hole burned in the Soret band is observed in the IR, and the enthalpic barrier distribution in the kinetic hole-burning experiments. The resulting perturbation of the distribution is measured along a different coordinate. Table 1 shows that the inhomogeneous width of the Soret band obtained by method 3 is one third that obtained by method 1. Thus, the mapping between the Soret spectral distribution and the enthalpic barrier distribution is not as simple as assumed. In the case of the A_1 band, both inhomogeneous widths involve assumptions about mapping of the two distributions. However, the total inhomogeneous broadening of A_1 obtained by method 4 is 2 cm^{-1} while method 2 results in a value three times smaller. The values indicate that the correlation between the distributions of the Soret and of the A_1 band is not very strong. We conclude that the spectral distribution of the A_1 band and $g(H)$ strongly depend on the same protein coordinate, while the spectral distribution of the Soret band is dominated by another coordinate. The mutual correlation of all of these distributions points to the complexity of the interactions among different parts of the protein. Fig. 7 summarizes the different distributions observed and their correlations.

The nonuniform mapping between the different distributions may also explain an apparent contradiction in the qualitative features of the results from the different methods. Since the spectral hole-burning experiment as observed in the IR (method 2) established a red-to-red and blue-to-blue correlation between the spectral distributions of the Soret and A_1 bands, one might think that both bands should shift in the same direction during kinetic hole-burning (methods 3 and 4). However, since the correlations among the distributions summarized in Fig. 7 are not very strong and different in the different cases, the opposite shift of the two peaks during rebinding of CO is not contradictory.

It has to be emphasized that while the Soret band reflects the whole MbCO population, the A_1 infrared band is characteristic of a CS^0 subpopulation of the molecules. In other words, the inhomogeneous broadening of the Soret includes CS^0, while that of band A_1 does not. This fact is illustrated in Fig. 1. Examination of the IR difference spectra of the hole-burning experiment monitored in the infrared (method 2) in the range of all A bands shows that the relative intensities of the A bands depend on the excitation wavelength (data not shown). The Soret band therefore is a sum of slightly shifted bands that belong to the three CS populations characterized by the A bands. The Soret band that corresponds to A_0 is shifted from that of A_1 by 0.4 ± 0.1 nm to the blue, while this value for A_3 is 0.6 ± 0.15 nm to the red.

The spectral hole-burning experiment monitored only

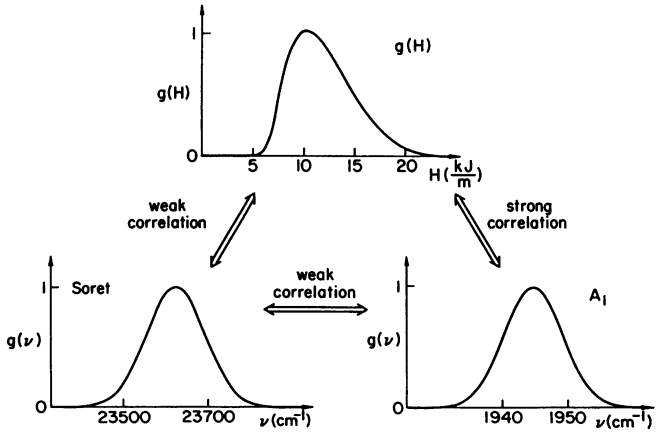

FIGURE 7 Summary of the spectral distributions and their correlations investigated in this work and their relation to the conformational substates and enthalpic barrier distribution $g(H)$.

in A_1 shows that the Soret band has inhomogeneous broadening also due to lower tiers (CS^1, CS^2, . . .); however, they are not resolved. At both CS^0 and lower tiers (CS^1, CS^2, . . .) the correlation between the spectral distribution in the Soret and A bands is such that high frequency in the visible corresponds to high frequency in the IR.

The structural marker: orientation of CO in MbCO

The infrared CO stretch bands have been used to determine the tilt angle α between the heme normal and the bound CO (13, 14). The method involves measurement of the linear dichroism after photoselection. The angle α provides a simple, direct parameter that characterizes the different A substates: $\alpha(A_0) = 15° \pm 3°$, $\alpha(A_1) = 28° \pm 2°$, $\alpha(A_3) = 33° \pm 4°$. The different A substates label proteins with slightly different structures near the heme pocket and, possibly, slightly different overall structures. Measurements with good signal-to-noise ratio show that the tilt angle is wave-number dependent in the A_0 and A_1 bands. (The effect probably also exists for the A_3 band). For example, the tilt angle of the A_1 band centered at 1,945 cm^{-1} changes from 26° at 1,940 cm^{-1} to 30° at 1,950 cm^{-1} (15). The spectral and functional heterogeneity of the A bands is thus coupled to a heterogeneity of the structure.

The results presented here suggest the following picture: Within a single CS^0 substate of MbCO, the distribution of enthalpic barriers, the distribution of stretch frequencies of bound CO, and the distribution of tilt angles of the bound CO are correlated. With this new insight into the characteristics of conformational substates in myoglobin, we move closer to the goal of understanding the relationship between the dynamic structure and function of proteins (15, 41).

We thank J. Berendzen, J. Bruce Johnson, Stan Luck, Alfons Schulte, and Aihua Xie for valuable discussions.

This work was supported in part by National Institutes of Health grants GM 18051 and GM 32455, National Science Foundation grant DMB87-16476, and Office of Naval Research grant N00014-89-K-0270.

Received for publication 10 July 1989 and in final form 22 September 1989

REFERENCES

1. Frauenfelder, H., G. A. Petsko, and D. Tsernoglou. 1979. Temperature-dependent x-ray diffraction as a probe of protein structural dynamics. *Nature* (*Lond.*). 280:558–563.
2. Cooper, A. 1981. Conformational fluctuation and change in biological macromolecules. *Sci. Prog. Oxford.* 66:473–497.
3. Petsko, G. A., and D. Ringe. 1984. Fluctuations in protein structure from x-ray diffraction. *Annu. Rev. Biophys. Bioeng.* 13:331–373.
4. Parak, F. 1987. A model of protein dynamics inferred from x-ray structure analysis and Mössbauer spectroscopy on myoglobin. *Mol. Cell. Biophys.* 4:265–280.
5. Austin, R. H., K. W. Beeson, L. Eisenstein, H. Frauenfelder, and I. C. Gunsalus. 1975. Dynamics of ligand binding to myoglobin. *Biochemistry.* 14:5355–5373.
6. Frauenfelder, H., F. Parak, and R. D. Young. 1988. Conformational substates in proteins. *Annu. Rev. Biophys. Biophys. Chem.* 17:451–479.
7. Ansari, A., J. Berendzen, D. Braunstein, B. R. Cowen, H. Frauenfelder, M. K. Hong, I. E. T. Iben, J. B. Johnson, P. Ormos, T. B. Sauke, R. Scholl, A. Schulte, P. J. Steinbach, J. Vittitow, and R. D. Young. 1987. Rebinding and relaxation in the myoglobin pocket. *Biophys. Chem.* 26:337–355.
8. Goldstein, M. 1969. Viscous liquids and the glass transition: a potential energy barrier picture. *J. Chem. Phys.* 51:3728–3739.
9. Palmer, R. G. 1982. Broken ergodicity. *Advan. Phys.* 31:669–735.
10. Mézard, M., G. Parisi, N. Sourlas, G. Toulouse, and M. Virasoro. 1984. Nature of the spin-glass phase. *Phys. Rev. Lett.* 52:1156–1159.
11. Binder, K., and A. P. Young. 1986. Spin glasses: experimental facts, theoretical concepts and open questions. *Rev. Mod. Phys.* 58:801–976.
12. Ansari, A., J. Berendzen, S. F. Bowne, H. Frauenfelder, I. E. T. Iben, T. B. Sauke, E. Shyamsunder, and R. D. Young. 1985. Protein states and proteinquakes. *Proc. Natl. Acad. Sci. USA.* 85:5000–5004.
13. Caughey, W. S., J. O. Alben, S. McCoy, S. H. Boyer, S. Carache, and P. Hathaway. 1969. Differences in the infrared stretching frequency of carbon monoxide bound to abnormal hemoglobins. *Biochemistry.* 8:59–62.
14. Makinen, M. W., R. A. Houtchens, and W. S. Caughey. 1979. Structure of carboxymyoglobin in crystals and in solution. *Proc. Natl. Acad. Sci. USA.* 78:6042–6046.
15. Ormos, P., D. Braunstein, H. Frauenfelder, M. K. Hong, S. -L. Lin, T. B. Sauke, and R. D. Young. 1988. Orientation of carbon monoxide and structure-function relationship in carbonmonoxy-myoglobin. *Proc. Natl. Acad. Sci. USA.* 85:8492–8496.
16. Moore, J. N., P. A. Hansen, and P. M. Hochstrasser. 1988. Iron-carbonyl bond geometries of carboxymyoglobin and carboxyhemoglobin in solution determined by picosecond time-resolved infrared spectroscopy. *Proc. Natl. Acad. Sci. USA.* 85:5062–5066.
17. Chance, M. R., B. F. Campbell, R. Hoover, and J. M. Friedman. 1987. Myoglobin recombination at low temperature. *J. Biol. Chem.* 262:6959–6961.
18. Frauenfelder, H. 1985. Ligand binding and protein dynamics. *In* Structure and Motion: Membranes, Nucleic Acids and Proteins. E. Clementi, G. Corongiu, M. H. Sarma, and R. H. Sarma, editors. Adenine Press, Guilderland, NY. 205–217.
19. Sauke, T. B. 1989. Long lived states induced by extended illumination of carbonmonoxy-myoglobin. Ph.D. thesis. University of Illinois at Urbana-Champaign, Urbana, IL.
20. Agmon, N. 1988. Reactive lineshape narrowing in low-temperature inhomogeneous germinate recombination of CO to myoglobin. *Biochemistry.* 27:3507–3511.

21. Campbell, B. F., M. R. Chance, and J. M. Friedman. 1987. Linkage of functional and structural heterogeneity in proteins: dynamic hole burning in carboxymyoglobin. *Science (Wash. DC.)*. 238:373–376.

22. Ansari, A. 1988. Conformational relaxation and kinetic hole burning in sperm whale myoglobin. Ph.D. thesis. University of Illinois at Urbana-Champaign, Urbana, IL.

23. Doster, W., S. Cusack, and W. Petry. 1989. Dynamical transition of myoglobin revealed by inelastic neutron scattering. *Nature (Lond.)*. 337:754–756.

24. Singh, G. P., H. J. Schink, H. Von Löhneysen, F. Parak, and S. Hunklinger. 1984. Excitations in metmyoglobin crystals at low temperatures. *Z. Phys.* B55:23–26.

25. Boxer, S. G., D. S. Gottfried, D. J. Lockhart, and T. R. Middendorf. 1987. Nonphotochemical hole burning in a protein matrix: chlorophyllide in apomyoglobin. *J. Chem. Phys.* 86:2439–2441.

26. Iben, I. E. T., D. Braunstein, W. Doster, H. Frauenfelder, M. K. Hong, J. B. Johnson, S. Luck, P. Ormos, A. Schulte, P. J. Steinbach, A. H. Xie, and R. D. Young. 1989. Glassy behavior of a protein. *Phys. Rev. Lett.* 62:1916–1919.

27. Hartmann, H., F. Parak, W. Steigemann, G. A. Petsko, D. Ringe-Ponzi, and H. Frauenfelder. 1982. Conformational substates in a protein: structure and dynamics of metmyoglobin at 80K. *Proc. Natl. Acad. Sci. USA.* 79:4967–4971.

28. Parak, F., and E. W. Knapp. 1984. A consistent picture of protein dynamics. *Proc. Natl. Acad. Sci. USA.* 81:7088–7092.

29. Cooper, A. 1983. Photoselection of conformational substates and the hypsochromic photoproduct of rhodopsin. *Chem. Phys. Lett.* 99:305–309.

30. Ormos, P., D. Braunstein, M. K. Hong, S-L. Lin, and J. Vittitow. 1986. Hole burning in bacteriorhodopsin. *In* Biophysical Studies of Retinal Proteins. T. G. Ebrey, H. Frauenfelder, B. Honig, and K. Nakanishi, editors. University of Illinois Press, Urbana, IL. 238–247.

31. Šrajer, V., K. T. Schomaker, and P. M. Champion. 1986. Spectral broadening in biomolecules. *Phys. Rev. Lett.* 57:1267–1270.

32. Ormos, P., A. Ansari, D. Braunstein, B. R. Cowen, H. Frauenfelder, M. K. Hong, I. E. T. Iben, T. B. Sauke, and R. D. Young. 1988. Inhomogeneous broadening in the Soret and ν(CO) IR bands of MbCO: the connection of the spectral and functional heterogeneity of sperm whale myoglobin. *Biophys. J.* 53:276*a*. (Absr.)

33. Frauenfelder, H. and P. Ormos. 1988. Protein dynamics and function. *In* Biological and Artificial Intelligence Systems. E. Clementi and S. Chin, ESCOM Press. 15–22.

34. Steinbach, P. J., H. Frauenfelder, J. B. Johnson, and T. B. Sauke. 1989. CO rebinding to sperm whale myoglobin: mapping the A substates into the Soret. *Biophys. J.* 55:565*a*. (Abstr.)

35. Hayes, J. M., and G. J. Small. 1978. Mechanisms of non-photochemical hole-burning in organic glasses. *Chem. Phys. Lett.* 54:435–438.

36. Jankowiak, R., and H. Baessler. 1983. Non-photochemical hole burning in tetracene-doped amorphous enthracene. *Chem. Phys. Lett.* 95:124–128.

37. Agmon, N., and J. Hopfield. 1983. CO binding to heme proteins: a model for barrier height distributions and slow conformational changes. *J. Chem. Phys.* 79: 2042–2053.

38. Rousseau, D. L. 1981. Raman difference spectroscopy as a probe of biological molecules. *J. Raman Spectrosc.* 10:94–99.

39. Batty, C. J., S. D. Hoath, and B. L. Roberts. 1976. Measurement of Lorentzian line-widths: numerical evaluation of the Voigt integral. *Nucl. Instrum. Methods.* 137:179–181.

40. Šrajer, V., L. Reinisch, and P. H. Champion. 1988. Protein fluctuations, distributed coupling, and the binding of ligands to heme proteins. *J. Am. Chem. Soc.* 110:6656–6666.

41. Frauenfelder, H., P. J. Steinbach, and R. D. Young. 1989. Conformational relaxation in proteins. *Chemica Scripta.* In press.